

Aggregation in Amphiphilic Macrocyclic-Substituted Gd^{3+} DOTA-Type Chelates Is Affected by the Regiochemistry of SubstitutionBenjamin C. Webber,[†] Claudio Cassino,[‡] Mauro Botta,^{*,‡} and Mark Woods^{*,†,§}[†]Department of Chemistry, Portland State University, 1719 SW 10th Avenue, Portland, Oregon 97201, United States[‡]Dipartimento di Scienze e Innovazione Tecnologica, Università del Piemonte Orientale "Amedeo Avogadro", Viale T. Michel 11, I-15121 Alessandria, Italy[§]Advanced Imaging Research Center, Oregon Health and Science University, 3181 SW Sam Jackson Park Road, Portland, Oregon 97239, United States

Supporting Information

ABSTRACT: Gd^{3+} chelates of macrocyclic bifunctional chelators (BFCs) can differentiate into two regioisomers: corner and side. These isomers afford different orientations of chelate relative to conjugate. These differences alter the self-assembly, tumbling, and effectiveness as magnetic resonance imaging contrast agents of the two biphenyl conjugate isomers.

Efforts to improve the effectiveness of Gd^{3+} -based contrast agents for magnetic resonance imaging (MRI) have largely been driven by the emergence of molecular imaging. Molecular imaging envisions the detection and mapping of biomolecules specific to disease through the use of imaging probes that selectively bind to these biomolecules. MRI offers one particular advantage for this type of application: it affords spatial resolution unsurpassed by other in vivo imaging modalities. MRI also has one particular drawback with respect to molecular imaging: the limits of detection of the contrast media employed are much higher than the concentrations of many of the biomolecules of interest. For this reason, it is imperative that as much image contrast be extracted per Gd^{3+} ion as possible. However, no Gd^{3+} chelate has yet exhibited the relaxivity (effectiveness) that some have calculated is possible according to Solomon, Bloembergen, and Morgan (SBM) theory.¹ This is in large part because certain assumptions made in these calculations are not universally valid.² This was not previously recognized because the vast majority of studies were undertaken on Gd^{3+} chelates with flexible coordination chemistries.¹ For these systems, multiple coordination species are present simultaneously in solution: the measured properties of the sample reflect a weighted average of these coordination species.³ This hampers the development of a truly accurate picture of relaxivity and how it is affected by the coordination chemistry of Gd^{3+} . We have taken a different approach, making the structure of the Gd^{3+} chelate rigid through substitution.^{4,5} In this way, it has been possible to definitively evaluate how changes in the chelate structure altered its effectiveness as an MRI contrast agent.^{6,7}

Previous studies^{4–7} have often focused on the difference between the two coordination isomers prevalent for all Gd-DOTA-type chelates (DOTA = 1,4,7,10-tetraazacyclododecane- N,N',N'',N''' -1,4,7,10-tetraacetate): the square antiprism (SAP) and twisted square antiprism (TSAP). It is well established that

the kinetics of water exchange between coordinated water and the bulk in the TSAP isomer are much faster than those in the SAP isomer.^{8,9} This had led to the conclusion that when incorporated into a molecular imaging probe, the TSAP isomer would afford the higher relaxivity of the two.¹⁰ However, our work demonstrated that this is not necessarily the case and that water exchange can quite easily be accelerated beyond the point at which it can afford maximum relaxivity.⁶ As part of these studies, we noted that substitution of the macrocyclic ring led to the formation of regioisomeric species in the same coordination geometry.^{11–13} We had denoted these two regioisomers as "corner" and "side" isomers, depending on the position of the benzylic substitution (Figure 1). In this report, we present preliminary findings into how this regioisomerism might affect the effectiveness of rigid Gd^{3+} chelates as MRI contrast agents. We have prepared both regioisomers of a Gd^{3+} chelate conjugated to a biphenyl modality (*S*-SSSS- Gd^{3+}), both frozen into TSAP coordination geometries (Chart 1).

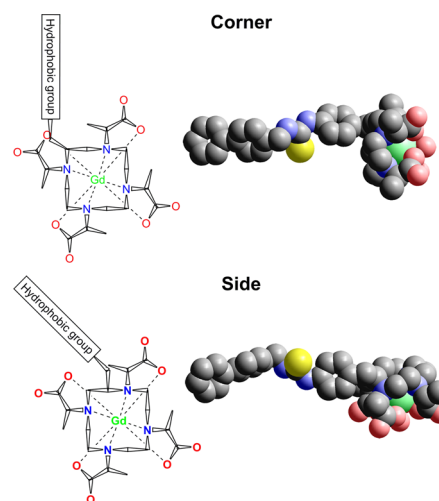
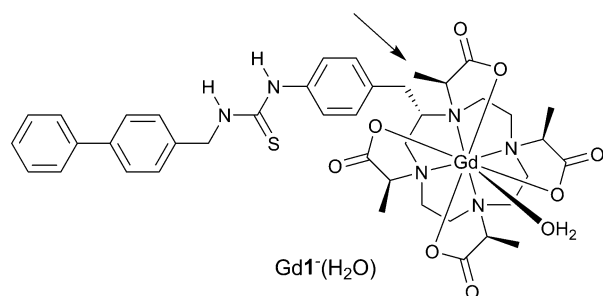


Figure 1. Wedge representations (left), following Dale's conventions,¹⁴ and space-filling models based on structural information provided by 2D NMR¹³ (right) of the corner (top) and side (bottom) isomers.

Received: December 1, 2014

Published: February 18, 2015

Chart 1. Structure of a Rigid DOTA-Derived Chelate, Gd-1⁻, Capable of Adopting only a TSAP Coordination Geometry^a



^aThe regiochemistry of the benzylic substituent is not discernible from a connectivity diagram. The arrow indicates the methyl substituent that was absent in our previous report on analogous chelates.⁶

The two regioisomeric chelates Gd-1⁻ closely resemble chelates frozen into SAP and TSAP geometries, which showed that faster water exchange does not always afford higher relaxivity.⁶ The difference between that study⁶ and this is the presence or absence of one methyl group (Chart 1). The chelates examined in the previous study were exclusively corner isomers.⁶ The ligand 1 was prepared according to previously reported methods⁶ (additional experimental details are provided in the Supporting Information, SI). The Gd³⁺ ion was introduced as the trichloride in excess at pH 6 in a 1:2 (v/v) dioxane/water solution. Each regioisomer of Gd-1⁻ was obtained as its acid from reversed-phase high-performance liquid chromatography purification of the chelation reaction mixture (8:5, corner/side). The colorless solid so obtained was found to be insoluble in water but was freely soluble when its Na⁺ salt was produced by the addition of sodium hydroxide.

NMR studies of the nitrobenzyl precursors to Gd-1⁻ have shown that the position of the benzylic substituent relative to the chelate is quite well-defined in this type of chelate.¹³ For the same regioisomer, very little difference is observed between the orientation of the benzylic group in the SAP and TSAP isomers. In contrast, significant differences are observed between the corner and side isomers. Molecular models of the chelates¹³ indicate, when biphenyl groups are conjugated, quite substantial differences between the conformation of the corner and side isomers of Gd-1⁻ (Figure 1). In the corner isomer, the hydrophobic group is angled behind the macrocyclic ring away from the hydrophilic face of the chelate. The side isomer is very different; the hydrophobic group is angled between the hydrophobic and hydrophilic faces of the chelate.

Consistent with previous observations,⁶ both regioisomers of Gd-1⁻ readily form micelles in solution. Micelle formation slows molecular tumbling and increases relaxivity. The longitudinal proton relaxation rate constant (R_1) of water is linearly dependent on the Gd³⁺ concentration for discrete chelates. However, measuring R_1 as a function of the Gd-1⁻ concentration affords a clear inflection point for both regioisomers (see the SI). This allows^{15–19} the critical micelle concentration (CMC), the concentration above which all amphiphiles are incorporated into micelles,²⁰ to be determined (Table 1). The CMCs of the two regioisomers are comparable but slightly higher for the corner isomer. Below the CMC, the concentration of micellar and aggregated amphiphiles decreases monotonically with decreasing Gd-1⁻ concentration.²⁰ This has two effects. It leads to a slight nonlinearity in the relationship between R_{1p} and [Gd-1⁻] (see

Table 1. CMCs and Relaxivities (20 MHz and 298 K) of the Two Regioisomers of Gd-1⁻

regioisomer	CMC (mM)	r_1 (mM ⁻¹ s ⁻¹)	
		above CMC	below CMC
Gd-1 ⁻ corner	0.24 (±0.01)	17.8 (±0.2)	10.0 (±0.1)
Gd-1 ⁻ side	0.21 (±0.01)	21.8 (±0.3)	8.0 (±0.1)

the SI). It also slightly increases the relaxivity measured below the CMC, which is not that of the discrete chelate. The measured relaxivities are higher than would be expected of chelates of modest size, such as these, and reflect the weighted average of all of the aggregation states in solution. Self-association below the CMC is evident from the nuclear magnetic relaxation dispersion (NMRD) profiles recorded at 298 K and 0.15 mM (Figure 2).

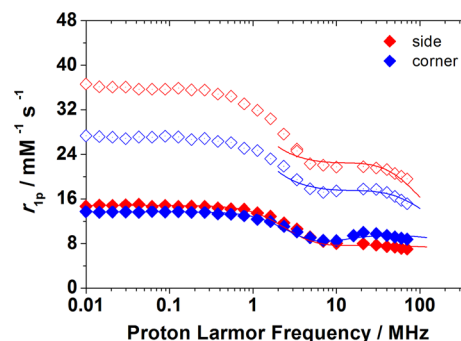


Figure 2. NMRD profiles of Gd-1⁻ corner (blue) and Gd-1⁻ side (red) isomers in aqueous solution (pH 7), 298 K, both at 0.4 mM, above the CMC (open symbols), and at 0.15 mM, below the CMC (closed symbols).

The small high-field humps observed between 10 and 50 MHz are characteristic of slower molecular tumbling (longer τ_R). The more pronounced hump and higher relaxivity of the corner isomer are consistent with more and/or stronger self-association below the CMC relative to the side isomer.

The relaxivity determined above the CMC is a direct measure of that of the chelate incorporated into a micelle. Upon incorporation into a micelle, the relaxivity of the side isomer is higher than that of the corner isomer, a reversal of the situation observed below the CMC. The NMRD profiles of both regioisomeric chelates incorporated into micelles exhibit high-field humps consistent with a long τ_R . Fitting these profiles to the SBM theory¹ incorporating the Lipari–Szabo model^{21,22} reveals that these micelles are more than large enough to slow the global tumbling of the chelate (τ_{RG}) enough that it no longer limits the relaxivity in either case ($\tau_{RG} \geq 1$ ns; Table 2).¹ The fitting parameters obtained from these profiles are comparable to those obtained for other cyclen-based Gd³⁺-containing micelle systems.^{15–19} Significantly, this is also the case for the electron-spin relaxation parameters Δ^2 (square of trace of zero-field splitting tensor) and τ_V (correlation time of its modulation), which differ significantly above and below the CMC. The values of these parameters above the CMC have no real physical meaning; low-field data, those most affected by electronic relaxation, were not included in data analysis.

Relaxivity in the micelles continues to be limited by the local rotation of the chelate (τ_{RL}). Analysis of the NMRD data reveals different rates of local motion for the corner and side isomers, which lead to different high-field relaxivities. These differences can be understood through a consideration of how the chelates

Table 2. Fitting Parameters for the NMRD Profiles in Figure 2^a

	below the CMC		above the CMC ^b	
	corner	side	corner	side
Δ^2 (10^{18} s ⁻²)	22 (± 1)	18 (± 1)	1.8 (± 0.3)	1.2 (± 0.2)
τ_V (ps)	25 (± 0.01)	21 (± 0.01)	10 (± 3)	10 (± 3)
τ_{RG} (ns)	250 (± 6)	187 (± 4)	1.9 (± 0.1)	2.1 (± 0.3)
τ_{RL} (ps)			470 (± 30)	520 (± 20)
S^2			0.35	0.46

^aParameters fixed during fitting were $q = 1$, $r_{GdH} = 3.1$ Å, $\tau_M = 10$ ns, $c = 4.0$ Å, and $^{298}D = 2.24 \times 10^{-3}$ cm²s⁻¹. ^bParameters were determined by the fitting data above 2 MHz only, consistent with previous practice.⁶ ^cIt was assumed that the water-exchange kinetics of the corner and side isomers of Gd-1⁻ were identical and fast; both isomers adopt TSAP geometries.

associate within the micelle (Figure 3). The negatively charged carboxylate surface of the corner isomer of the chelate is oriented

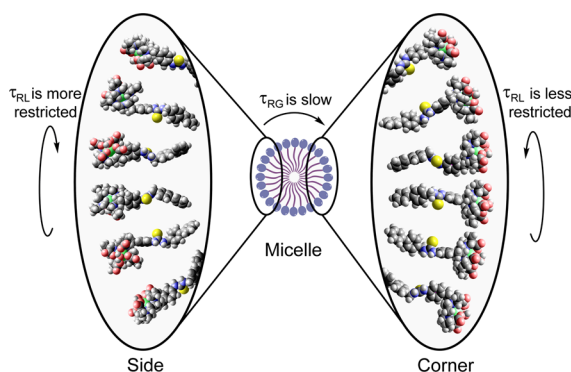


Figure 3. Schematic representation of the orientation of each isomeric chelate once incorporated into a micelle.

away from the micelle, and the local rotation of the chelate would not bring these surfaces of two chelates closer together. In contrast, the negatively charged carboxylate surface of the side isomer of the chelate is oriented sideways, and one can envision that the local rotation of this chelate might tend to bring these surfaces in closer proximity. This would be expected to increase the energy barrier to the local rotation for this isomer, making τ_{RL} longer and increasing relaxivity.

These results point directly to important differences arising from the structural variations associated with the regiochemistry of substitution in macrocyclic Gd³⁺ chelates. These structural variations directly affect the way in which the chelates are able to self-associate in solution. These differences affect how each chelate tumbles on a global and local level. These differences are reflected in their relaxivities, which are significant on a per Gd³⁺ basis. However, if these agents were to be used, as may be envisioned, in the context of nanoscale molecular imaging probes incorporating many thousands of chelates per agent, then the multiplicative effect of these differences could be huge.

■ ASSOCIATED CONTENT

📄 Supporting Information

Experimental details, determination of the CMC, and calculation of the electron-spin relaxation parameters. This material is available free of charge via the Internet at <http://pubs.acs.org>.

■ AUTHOR INFORMATION

Corresponding Authors

*E-mail: mauro.botta@unipmn.it.

*E-mail: mark.woods@pdx.edu or woodsmar@ohsu.edu.

Notes

The authors declare no competing financial interest.

■ ACKNOWLEDGMENTS

M.B. is thankful for financial support of the “Compagnia di San Paolo” (Project CSP-2012 NANOPROGLY).

■ REFERENCES

- (1) Caravan, P.; Ellison, J. J.; McMurry, T. J.; Lauffer, R. B. *Chem. Rev.* **1999**, *99*, 2293.
- (2) Webber, B. C.; Woods, M. *Dalton Trans.* **2014**, *43*, 251.
- (3) Aime, S.; Botta, M.; Garda, Z.; Kucera, B. E.; Tircsó, G.; Young, V. G.; Woods, M. *Inorg. Chem.* **2011**, *50*, 7955.
- (4) Woods, M.; Botta, M.; Avedano, S.; Wang, J.; Sherry, A. D. *Dalton Trans.* **2005**, 3829.
- (5) Woods, M.; Kovacs, Z.; Zhang, S.; Sherry, A. D. *Angew. Chem., Int. Ed.* **2003**, *42*, 5889.
- (6) Avedano, S.; Botta, M.; Haigh, J. S.; Longo, D. L.; Woods, M. *Inorg. Chem.* **2013**, *52*, 8436.
- (7) Borel, A.; Bean, J. F.; Clarkson, R. B.; Helm, L.; Moriggi, L.; Sherry, A. D.; Woods, M. *Chem.—Eur. J.* **2008**, *14*, 2658.
- (8) Woods, M.; Aime, S.; Botta, M.; Howard, J. A. K.; Moloney, J. M.; Navet, M.; Parker, D.; Port, M.; Rousseaux, O. *J. Am. Chem. Soc.* **2000**, *122*, 9781.
- (9) Aime, S.; Barge, A.; Bruce, J. I.; Botta, M.; Howard, J. A. K.; Moloney, J. M.; Parker, D.; de Sousa, A. S.; Woods, M. *J. Am. Chem. Soc.* **1999**, *121*, 5762.
- (10) Siriwardena-Mahanama, B. N.; Allen, M. J. *Molecules* **2013**, *18*, 9352.
- (11) Tircsó, G.; Webber, B. C.; Kucera, B. E.; Young, V. G.; Woods, M. *Inorg. Chem.* **2011**, *50*, 7966.
- (12) Slack, J. R.; Woods, M. *J. Biol. Inorg. Chem.* **2014**, *19*, 173.
- (13) Webber, B. C.; Woods, M. *Inorg. Chem.* **2012**, *51*, 8576.
- (14) Dale, J. *Acta Chem. Scand.* **1973**, *27*, 1115.
- (15) Nicolle, G. M.; Toth, E.; Eisenwiener, K.-P.; Macke, H. R.; Merbach, A. E. *J. Biol. Inorg. Chem.* **2002**, *7*, 757.
- (16) Schuhle, D. T.; Schatz, J.; Laurent, S.; Vander Elst, L.; Muller, R. N.; Stuart, M. C. A.; Peters, J. A. *Chem.—Eur. J.* **2009**, *15*, 3290.
- (17) Torres, S.; Martins, J. A.; Andre, J. P.; Geraldes, C. F. G. C.; Merbach, A. E.; Toth, E. *Chem.—Eur. J.* **2006**, *12*, 940.
- (18) Vanasschen, C.; Bouslimani, N.; Thonon, D.; Desreux, J. F. *Inorg. Chem.* **2011**, *50*, 8946.
- (19) Ferreira, M. F.; Pereira, G.; Martins, A. F.; Martins, C. I. O.; Prata, M. I. M.; Petoud, S.; Toth, E.; Ferreira, P. M. T.; Martins, J. A.; Geraldes, C. F. G. C. *Dalton Trans.* **2014**, *43*, 3162.
- (20) Ruckenstein, E.; Nagarajan, R. *J. Phys. Chem.* **1975**, *79*, 2622.
- (21) Lipari, G.; Szabo, A. *J. Am. Chem. Soc.* **1982**, *104*, 4546.
- (22) Lipari, G.; Szabo, A. *J. Am. Chem. Soc.* **1982**, *104*, 4559.